

Protein mutated in paroxysmal dyskinesia interacts with the active zone protein RIM and suppresses synaptic vesicle exocytosis

Yiguo Shen^{a,1}, Woo-Ping Ge^{b,2}, Yulong Li^{c,3}, Arisa Hirano^a, Hsien-Yang Lee^a, Astrid Rohlmann^d, Markus Missler^d, Richard W. Tsien^{c,4}, Lily Yeh Jan^{b,e}, Ying-Hui Fu^{a,5}, and Louis J. Ptáček^{a,e,5}

^aDepartment of Neurology, ^bDepartment of Physiology, and ^cHoward Hughes Medical Institute, University of California, San Francisco, CA 94158; ^dDepartment of Cellular & Molecular Physiology, Stanford University, Palo Alto, CA 94304; and ^eInstitute of Anatomy and Molecular Neurobiology, Westfälische Wilhelms-University & Cluster of Excellence EXC 1003, Cells in Motion, D-48149 Münster, Germany

This contribution is part of the special series of Inaugural Articles by members of the National Academy of Sciences elected in 2012.

Contributed by Louis J. Ptáček, January 22, 2015 (sent for review November 1, 2014)

Paroxysmal nonkinesigenic dyskinesia (PNKD) is an autosomal dominant episodic movement disorder precipitated by coffee, alcohol, and stress. We previously identified the causative gene but the function of the encoded protein remains unknown. We also generated a PNKD mouse model that revealed dysregulated dopamine signaling in vivo. Here, we show that PNKD interacts with synaptic active zone proteins Rab3-interacting molecule (RIM)1 and RIM2, localizes to synapses, and modulates neurotransmitter release. Overexpressed PNKD protein suppresses release, and mutant PNKD protein is less effective than wild-type at inhibiting exocytosis. In PNKD KO mice, RIM1/2 protein levels are reduced and synaptic strength is impaired. Thus, PNKD is a novel synaptic protein with a regulatory role in neurotransmitter release.

paroxysmal dyskinesia | exocytosis | neurological disease

Paroxysmal nonkinesigenic dyskinesia (PNKD)* is a rare dominantly inherited episodic movement disorder. First reported in 1940 (1), PNKD is characterized by childhood onset with involuntary movements in the limbs, trunk, and face manifesting as dystonia, chorea, and athetosis (2). PNKD shows nearly complete penetrance and attacks are precipitated by fatigue, stress, hunger, and consumption of coffee or alcohol. Patients are completely normal between attacks.

Hereditary forms of many episodic disorders are recognized and include movement disorders, muscle diseases, cardiac arrhythmias, epilepsy, and headache. A majority of the causative genes that have been identified encode ion channels (3). Studies in several spontaneous mouse mutants with a paroxysmal dyskinesia phenotype have provided intriguing insights into these otherwise complicated diseases (4–6). The *tottering* and *lethargic* mice display motor abnormalities mimicking paroxysmal dyskinesia and harbor mutations in the genes encoding the $\alpha 1A$ and $\beta 4$ subunits of the P/Q-type voltage-gated Ca^{2+} -channel, respectively (7, 8). Like PNKD, the dyskinesia phenotype in *tottering* mice can also be triggered by caffeine and stress. PNKD is interesting in that the gene encodes a novel protein with homology to human glyoxalase II, an enzyme in a stress-response pathway. Although the normal role of PNKD is unknown, we previously identified the causative gene of PNKD (9) and a mouse model of the human mutations recapitulates the phenotype and shows dopamine signaling dysregulation (10).

At synapses, vesicle priming, docking, and fusion at synaptic terminals are complex and coordinately regulated by proteins from the active zone, presynaptic membrane, and vesicles (11). Rab3-interacting molecules (RIMs) are a family of active zone proteins encoded by genes, *Rims 1 to 4* (12). Through their interactions with vesicle proteins, active zone proteins, and presynaptic membrane proteins, RIMs are centrally involved in basic parameters of neurotransmitter release, and they contribute to both long-term and short-term synaptic plasticity (13–18).

Given that PNKD is a novel protein whose function is unknown, we set out to identify proteins that interact with PNKD to provide clues to its normal function. Here, we show that PNKD is a novel synaptic protein that interacts with RIMs and can be found at presynaptic terminals. RIM1 and RIM2 are known to facilitate exocytosis and wild-type PNKD protein inhibits the RIM-dependent increase of neurotransmitter release. Mice deficient in *Pnkd* have decreased RIM levels, impaired synaptic facilitation and transmission, and abnormal motor behavior. Thus, PNKD is a novel synaptic protein regulating exocytosis in vitro and in vivo.

Results

PNKD Interacts with RIM1 and RIM2 and Localizes to Synapses. The PNKD long isoform (PNKD-L) is CNS-specific and localizes to the cell membrane in vitro. To identify the proteins with which *Pnkd* interacts, we immunoprecipitated *Pnkd*-L from C57BL/6

Significance

Paroxysmal nonkinesigenic dyskinesia (PNKD) is an autosomal dominant episodic movement disorder precipitated by coffee, alcohol, and stress. Here, we show that PNKD interacts with synaptic active zone proteins Rab3-interacting molecule (RIM)1 and RIM2, localizes to synapses, and modulates neurotransmitter release. PNKD knockout mice have impaired synaptic transmission and short-term plasticity.

Author contributions: Y.S., Y.-H.F., and L.J.P. designed research; Y.S., W.-P.G., Y.L., A.H., A.R., M.M., R.W.T., and L.Y.J. performed research; H.-Y.L. contributed new reagents; Y.S., W.-P.G., Y.L., A.H., A.R., M.M., R.W.T., and L.Y.J. analyzed data; and Y.S., Y.-H.F., and L.J.P. wrote the paper.

The authors declare no conflict of interest.

Freely available online through the PNAS open access option.

¹Present address: Nvigen, Inc., Santa Clara, CA 95054.

²Present address: Department of Pediatrics and Neurosciences, Children's Medical Center Research Institute, University of Texas Southwestern Medical Center, Dallas, TX 75390.

³Present address: Peking-Tsinghua Center of Life Sciences, School of Life Science, Peking University, Beijing 100871, China.

⁴Present address: Department of Physiology and Neuroscience, New York University Neuroscience Institute, New York University Langone Medical Center, New York, NY 10016.

⁵To whom correspondence may be addressed. Email: ying-hui.fu@ucsf.edu or ljp@ucsf.edu.

This article contains supporting information online at www.pnas.org/lookup/suppl/doi:10.1073/pnas.1501364112/-DCSupplemental.

*Standard nomenclature for names of genes and proteins are used in the paper. In vitro experiments were performed in cells transfected with the human cDNA and in vivo experiments were done in mice. The nomenclature is confusing because the naming of human genes/proteins is different and because the official gene names are the same as the acronym for this disorder. Throughout the report we use the terms as follows: PNKD is the acronym for the disorder, *PNKD* is the human gene, *Pnkd* is the mouse gene, and *Pnkd* is the mouse protein. In cases referring to both human and mouse gene/protein, such as "In vitro and in vivo data support a role for PNKD. . . ." we have used the human gene/protein name.

mouse frontal cortex homogenates using an antibody raised against a C-terminal peptide. *Pnkd*^{-/-} mice were used as a negative control. Proteins that coimmunoprecipitated with Pnkd-L were resolved on an SDS/PAGE gel, visualized by silver-staining, and analyzed by mass spectrometry. RIM2 sequences were identified from one protein band of ~150 kD (Fig. S1A and Table S1). This band was present in extracts from wild-type and mutant transgenic (mut-Tg) mice but not from PNKD KO mice. We then used a nonspecific anti-RIM antibody and confirmed that both RIM1 and RIM2 were pulled down by Pnkd from wild-type but not *Pnkd*^{-/-} mouse frontal cortex homogenates (Fig. 1A and Fig. S1B). The vesicular GTPase Rab3 and the S/M-protein Munc18 were not precipitated, underlining the specificity of the interaction (Fig. S1C). To further address the interaction of PNKD with RIMs, we coexpressed PNKD with full-length RIM1 or RIM2, or polypeptides encompassing individual domains (zinc finger, PDZ, C2A, or C2B) in HEK293 cells by coimmunoprecipitation. Wild-type PNKD protein interacts with RIM1, RIM2 (Fig. 1B), and the polypeptides containing only the C2B domain (Fig. 1C). This interaction was much weaker when PNKD protein harboring both of the human mutations (A7V/A9V) was used for the pull down. PNKD also showed very weak affinity for the amino-terminal polypeptide of RIMs for both the wild-type and mutant.

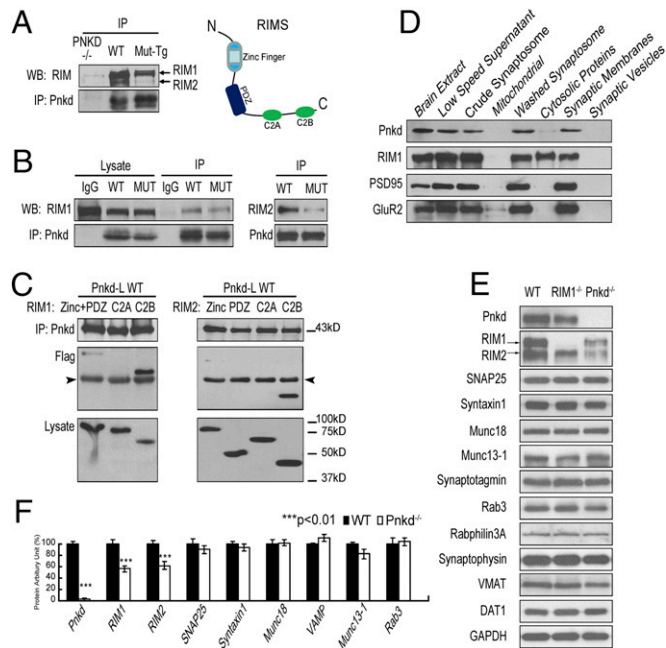


Fig. 1. PNKD interacts with RIMs and *Pnkd* knockout mice have lower RIM protein levels. (A) In mouse frontal cortex homogenates, RIM1 and RIM2 proteins coimmunoprecipitated with Pnkd but were not pulled down in homogenates from *Pnkd*^{-/-} mice (negative control). Protein domains of RIM are shown schematically at the right. (B) When wild-type or mutant PNKD was coexpressed with RIM1 or RIM2 in HEK293 cells and immunoprecipitated with rabbit IgG or anti-PNKD antibody, RIMs were pulled down. The interaction was weaker for mutant PNKD vs. wild-type. (C) DNA fragments encoding specific protein domains of RIM1 (Left) and RIM2 (Right) were subcloned and tested for interaction with wild-type PNKD. Arrowheads mark a nonspecific band. (D) Brain (frontal cortex) homogenates fractionated on a sucrose gradient and immunoblotted with antibodies to synaptic proteins to identify different fractions. PNKD sediments with the synaptic membrane fraction. (E) Representative immunoblots of synaptic proteins in frontal cortex homogenates of adult wild-type, RIM1^α-, and *Pnkd*^{-/-} mice. The RIM antibody cross-reacts with both RIM1 and RIM2. GAPDH was used as loading control. (F) Relative levels of synaptic proteins in WT and *Pnkd*^{-/-} mouse frontal cortex, normalized to GAPDH. Pnkd, RIM1, and RIM2 are the only proteins that are significantly decreased in *Pnkd*^{-/-} mouse brain. See also Fig. S1 and Table S1.

Because RIMs are synaptic proteins and localize to the presynaptic active zone, the sites of synaptic vesicle release, we tested whether Pnkd also localizes to synapses. Using differential and sucrose gradient centrifugation, synaptosome proteins from mouse cortex homogenates were separated into vesicular, cytosolic, synaptic membrane, and mitochondrial fractions. Pnkd was detected in the synaptic membrane fraction along with RIM and GluR2 proteins (Fig. 1D). To study the functional role of Pnkd protein in vivo, we generated a *Pnkd*-null mouse line (10). The homozygous *Pnkd*^{-/-} mice are viable, with normal body weight and no gross morphologic abnormalities (Fig. S1D–F). We next compared the protein levels of synaptic proteins in *Pnkd*^{-/-} mice and wild-type littermates. In frontal cortex homogenates, both RIM1 and RIM2 protein levels are significantly reduced in *Pnkd*^{-/-} mice, whereas other synaptic proteins examined were unchanged (Fig. 1E and F). We then tested whether the PNKD protein alters the stability of RIM. We found that RIM1 degradation was slower when cotransfected with either wild-type or mutant PNKD in a neuroblastoma cell line after cyclohexamide treatment (Fig. S1G). This finding suggests that the decreases of RIM1 and RIM2 levels in *Pnkd*^{-/-} mice were caused by RIM protein destabilization.

Proteins that interact with RIMs in vesicle priming, such as Munc13-1 and Rab3, were not changed. To evaluate if the reduced levels of RIM proteins in the PNKD KO mice had any functional consequences, we probed basic behaviors. Although PNKD-deficient mice did not reveal the caffeine-induced hyperkinetic movements typical for the disease-associated mutations (10), we tested *Pnkd*^{-/-} mice ($n = 7$) and their wild-type littermates ($n = 11$) on a rotarod to evaluate normal motor function. *Pnkd*^{-/-} mice showed shorter latency to fall from the rotating wheel than their wild-type littermates in each trial, demonstrating impairment of motor function (Fig. S1H).

The unexpected interaction of PNKD with RIM proteins suggests that their pathways intersect at the synapse. A previous investigation demonstrated specific expression of PNKD in neuronal subpopulations at the light microscopical level (9). We used immunogold electron microscopy to probe the ultrastructural localization of endogenous Pnkd in cortical tissue of adult mice, including the same region used for our initial pull-down experiments. To distinguish between bona fide localization and residual background from the polyclonal antiserum 2226, we compared labeling patterns in wild-type and *Pnkd*^{-/-} samples as negative control. PNKD localizes to the presynaptic terminal (Fig. 2A₁ and A₂), including the active zone between the inner side of the presynaptic membrane and synaptic vesicles where RIMs act (17, 19). In addition, PNKD can also be found in postsynaptic regions and over mostly membranous structures in dendrites (Fig. 2B). Control labelings of wild-type samples without first antibody were essentially devoid of gold particles (Fig. 2C), but some residual background staining with antibody 2226 remained on sections from PNKD-deficient animals (Fig. 2D). Because virtually no labeling of presynaptic profiles was found in *Pnkd*^{-/-} samples (Fig. 2D), we conclude from these data that the anti-PNKD antiserum 2226 reliably detects the protein at synapses. Taken together, these data indicate that PNKD is a synaptic protein, that it localizes to the pre- and postsynaptic terminals, and that it interacts with cytomatrix active zone RIM proteins through the C2B domain.

PNKD Inhibits Exocytosis Through a RIM-Dependent Pathway. Because *PNKD* encodes a synaptic protein widely expressed in neurons and at synapses of the CNS, we thus performed in vitro experiments to test whether PNKD plays a role in synaptic vesicle exocytosis. We used a vesicular pH-sensitive GFP indicator (VGluT1-pHluorin) to directly visualize and assay neurotransmitter release in cultured rat primary hippocampal neurons. During electrical stimulation, action potential evoked transmitter release led to a transient increase of fluorescence signal reflection that corresponds to the externalization of the luminal domain of the vesicular glutamate transporter. We used 10-Hz

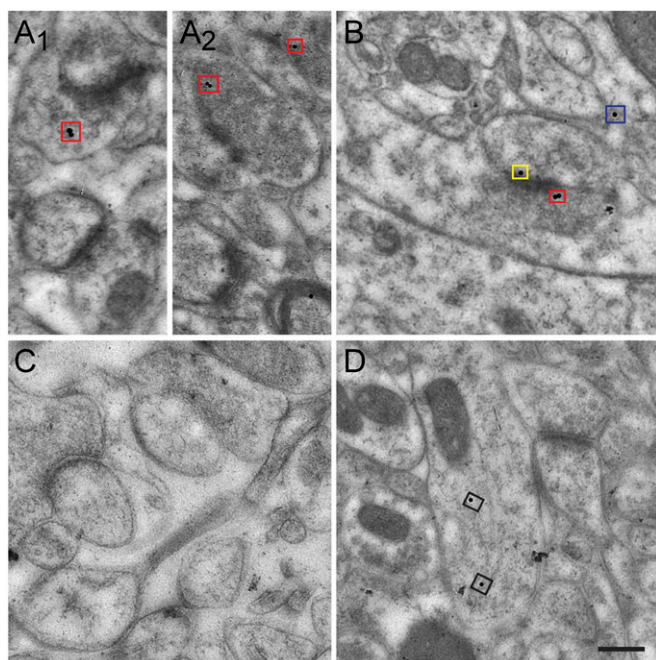


Fig. 2. *Pnkd* localizes to synaptic terminals. Lowicryl postembedding electron microscopy was applied to localize PNKD in the neocortex of wild-type and *Pnkd*^{-/-} mice. (A₁ and A₂) Representative images of immunolabeling show gold particles (boxed in red) in the presynaptic terminal filled with synaptic vesicles. (B) In addition to presynaptic localization (red) PNKD is also found in postsynaptic profiles (boxed in yellow), and dendrites (boxed in blue). (C) Omission of first antibody exhibits virtually no labeling with gold-coupled secondary antibodies under otherwise identical conditions. (D) Control experiments in samples from *Pnkd*^{-/-} animals do not reveal labeling of presynaptic terminals but contain some residual staining in other cellular compartments (black boxes in dendritic profile). (Scale bar in D for all panels, 100 nm.)

stimulation for 30 s to assay part of the total recycling pools. Overexpressed wild-type PNKD significantly reduces neurotransmitter release to 50% that of controls transfected with empty vector (Fig. 3 A and B). Because mutant PNKD fails to suppress vesicle release in our assay (Fig. 3 A and B) but also binds less well to RIM2 (Fig. 1 A and B), it can be hypothesized that RIM2 is particularly important to mediate the PNKD effect on release. The fluorescent decay time constant, a surrogate for endocytosis rate, did not change with either wild-type or mutant PNKD overexpression (Fig. 3C). These results collectively point to a model where PNKD antagonizes the action of RIM in modulation of synaptic transmitter release.

Synaptic Facilitation Is Impaired in *Pnkd*^{-/-} Mice. We examined synaptic electrophysiological properties of *Pnkd*^{-/-} mice in hippocampal CA1 Schaffer collateral excitatory synapses. Synaptic strength (input-output ratio) is significantly weakened in *Pnkd*^{-/-} mice, compared with the field excitatory postsynaptic potential (fEPSP) slope (output) vs. fiber volley (input) (Fig. 4A and Fig. S3). Paired-pulse facilitation is a measure of synaptic short-term plasticity that is typically inversely correlated with release probability. In line with the change in synaptic strength (Fig. 4A), paired-pulse facilitation was significantly increased at short interstimulus intervals (ISI) (Fig. 4B). Accordingly, synaptic facilitation of *Pnkd*^{-/-} mice was also significantly increased in response to short stimulus trains. When stimulated at 5 or 10 Hz, *Pnkd*^{-/-} mice show significantly higher field potentials after the third stimulus, but at stimulus trains of a lower frequency (1 Hz) show no significant differences (Fig. 4 C–F). The weakened synaptic strength and increased synaptic facilitation in paired-pulse and trains in *Pnkd*^{-/-} mice is qualitatively similar to that of mice

deficient in RIM proteins (15–17), consistent with lower RIM1 protein levels in the *Pnkd*^{-/-} cortex.

In addition to synaptic facilitation, we also studied the miniature excitatory postsynaptic currents (mEPSC) in *Pnkd*^{-/-} and wild-type mice to look for possible synaptic alterations under basal conditions. We did not detect significant differences in the frequency and amplitude of mEPSCs between PNKD KO and wild-type neurons (Fig. 4 G–I), although a tendency for a somewhat lower frequency existed. This result might be explained by the fact that mEPSCs only reflect the basic activity of neuronal transmission. We did not detect significant difference in evoked neuronal transmission at 1 Hz between PNKD KO and wild-type (Fig. 4D). The difference between KO and wild-type neurons is likely only able to be uncovered under stressful conditions, such as 5 Hz, 10 Hz, or with higher-frequency stimuli (Fig. 4 E and F).

Discussion

PNKD Is a Novel Synaptic Protein That Modulates RIM Function. Neurons signal through complex cascades of events, including presynaptic neurotransmitter release, postsynaptic receptor activation, ion channel opening, depolarization, signal propagation along axons, and calcium/voltage-triggered neurotransmitter release from downstream synapses. There are many examples of mutant ion channel genes causing episodic neurological phenotypes as a result of alterations of physiological properties of these proteins (3). However, altered function of elements all along this signaling cascade could have detrimental effects on CNS signaling and give rise to electrical disorders (20). In vivo data from the *Pnkd*^{-/-} mice and the identification of RIM1 and RIM2 as *Pnkd*-binding proteins focused attention on a potential role of *Pnkd* in synaptic regulation.

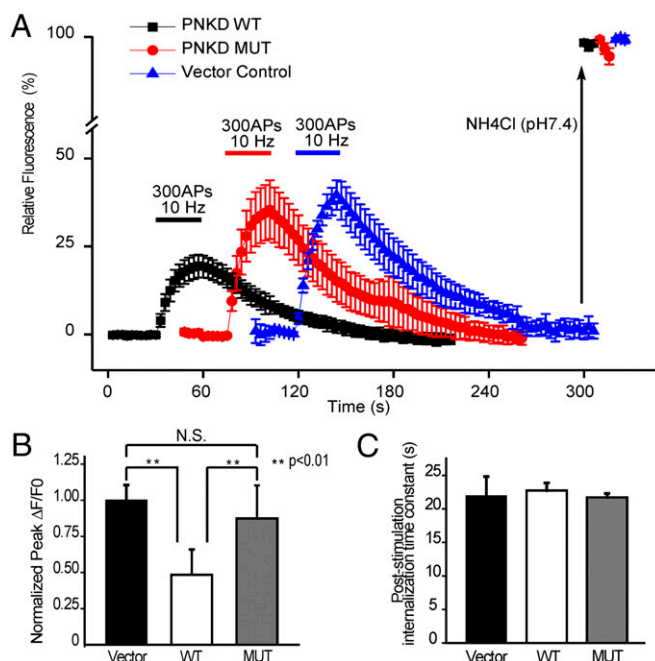


Fig. 3. PNKD suppresses exocytosis. (A) Time course of fluorescence signal changes of VGLUT1-pHluorin during and after 10-Hz stimulation for 30 s. Cultured rat primary neurons were cotransfected with wild-type or mutant PNKD-mKate or empty vector. Total VGLUT1-pHluorin was normalized to NH₄Cl treatment, *n* = 3 coverslips, 100–200 boutons per coverslip. Traces of wild-type, MUT, and vector control were intentionally separated on the x axis for ease of viewing. (B) Peak ΔF (normalized to total VGLUT1-pHluorin pool) shows a reduction in cells expressing wild-type PNKD, but MUT PNKD did not (***P* < 0.01, Student *t* test). (C) Poststimulation endocytosis time constants were derived by fitting with a single exponential function. No difference was found for wild-type or MUT PNKD vs. empty vector. See also Fig. S2.

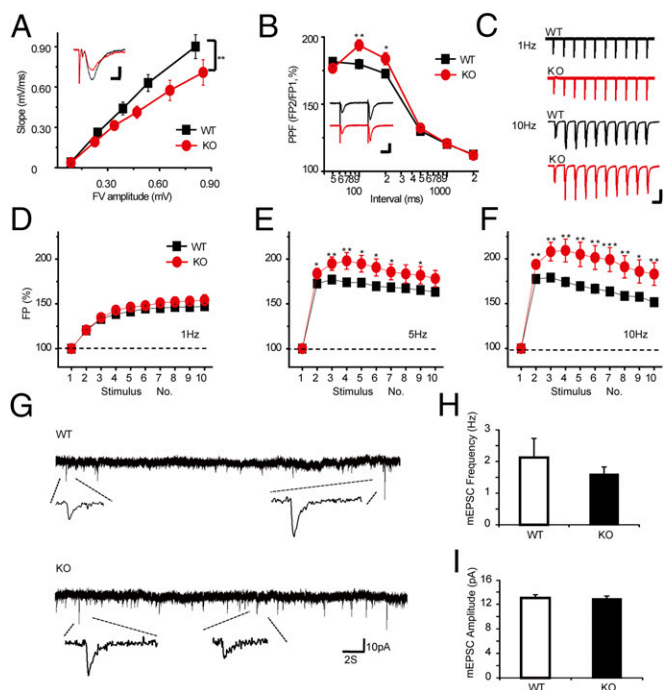


Fig. 4. Synaptic facilitation defects in *Pnkd* knockout mice. Hippocampus Schaffer collateral CA1 excitatory synapses and motor cortical mEPSCs are studied. (A) The fEPSP slopes are plotted to the afferent fiber volley amplitude. Linear fit slopes for wild-type ($k = 1.26 \pm 0.10$, $r = 0.98$, 6 mice, 19 slices) and *Pnkd*^{-/-} mice ($k = 0.84 \pm 0.08$, $r = 0.97$, 5 mice, 11 slices) are significantly different ($P < 0.01$, Student *t* test). (Scale bar, 0.5 mV, 10 ms.) (B) Paired-pulsed facilitation (fEPSP₂/fEPSP₁) are plotted to the ISI for wild-type (6 mice, 16 slices) and *Pnkd*^{-/-} mice (5 mice, 10 slices). Two traces represent wild-type and *Pnkd*^{-/-} at 0.2-s ISI. (Scale bar, 0.5 mV, 25 ms.) (C–F) Synaptic plasticity measured during 1-, 5-, and 10-Hz stimulus trains. Traces are field potential (FP) of wild-type and *Pnkd*^{-/-} mice under 1- and 10-Hz trains, representatively. (Scale bar, 0.4 mV, 100 ms/1 s.) (C). FP values are normalized to the first synaptic response of the train and plotted as a function of stimulation numbers in the train. Significant differences were noted at 5 Hz (E) and 10 Hz (F) in wild-type (6 mice, 19 slices) vs. *Pnkd*^{-/-} (5 mice, 11 slices) mice. See also Fig. S3. (G–I) The mEPSC were recorded in pyramidal neurons in layer 2–3 of motor cortical brain slices freshly prepared from 3-wk-old PNKD KO and wild-type mice (KO, $n = 15$ neurons; wild-type, $n = 14$ neurons, three to five mice for each group). Two mEPSC traces from wild-type and *Pnkd*^{-/-} preparations are shown (G). No significant difference in frequency (H) and amplitude (I) of mEPSC was found between PNKD KO and WT neurons.

RIM1 and RIM2 are large multidomain scaffold proteins that reside in the presynaptic active zone and are composed of an N-terminal α -helical region that is followed by a zinc finger domain, a central PDZ domain, and two C-terminal C2 domains (C2A and C2B) that do not bind Ca^{2+} (Fig. 1A). Each domain associates with specific binding partners, positioning RIM1 and RIM2 as central nodes for organizing release. The N-terminal region forms a tripartite complex with Rab3 and Munc13 that orchestrates synaptic vesicle priming (17, 18, 21–24). The central PDZ-domain binds to the active zone protein ELKS (25–27), and it tethers N- and P/Q-type Ca^{2+} channels to the active zone by forming a tripartite complex with α -subunits of P/Q- and N-type Ca^{2+} channels and RIM-binding protein (16, 28, 29). The functions of the C-terminal RIM C2-domains during release are less well understood. They have been shown to associate in vitro with liprin- α , synaptosomal-associated protein 25 (SNAP 25), synaptotagmin 1, with additional subtypes of Ca^{2+} -channels (17, 30, 31), and they may be regulated by the E3 ubiquitin ligase Scrapper (32). Through these multi-interaction domains, RIMs function as a central hub in connecting presynaptic proteins that are spatially heterogeneous and play an essential role in vesicle priming and calcium-dependent release.

RIM1 and RIM2 are functionally redundant; whereas single isoform knock-outs survive, removing multiple RIM isoforms strongly impairs survival (15–17, 19).

Here, we show that PNKD interacts with the C2B domain of RIM1/2 and inhibits neurotransmitter release (Fig. S4). Loss-of-function of RIM (unc10) in *Caenorhabditis elegans* results in synaptic priming defects and cannot be rescued by unc10 with the C2B-deletion, indicating an important functional role for the C2B domain at the active zone (24). Our experiments show that PNKD is required for normal RIM levels. In the PNKD KO animals, RIM levels are significantly reduced, and the PNKD KO phenotype is qualitatively similar to a loss of RIM phenotype, although less severe. Thus, PNKD may have a role in stabilizing RIMs at the active zone. On the other hand, overexpressed PNKD inhibits exocytosis, but it is currently not clear whether this effect operates through RIM or through unknown interacting proteins. Our data are consistent with suppression of exocytosis either through RIM by modulation of the N-terminal priming complex (22, 23) or of the Ca^{2+} -channel tethering complex (16), or through unknown interactors in the nerve terminal. We propose a model wherein PNKD stabilizes RIM and inhibits the RIM-dependent pathway to suppress presynaptic neurotransmitter release. Interestingly, although RIM1 and RIM2 are functionally redundant, they show different expression patterns (19). This finding suggests that PNKD functions through redundant pathways and unique functions may result from specific interactions of different partners with the individual domains of PNKD. Consistent with its role in synapse function and further validating the physiological significance of its binding to RIM, we show that the ultrastructural localization of PNKD includes specific presence in presynaptic terminals, which is not found in *Pnkd*^{-/-} samples (Fig. 2). At the same time, expression of PNKD in the postsynapse and other neuronal compartments suggests that the role of this protein is not only limited to exocytosis of synaptic vesicles.

Although the normal function of PNKD appears to be stabilization of RIM proteins, at least in part, the PNKD protein harboring human mutations does not lead to reduced RIM protein levels. This finding is consistent with the mutations leading to PNKD through a gain-of-function mechanism, as we have previously shown (10). Thus, the mutations are exerting an effect via a mechanism different from reducing RIM protein expression. This finding also fits with the fact that we saw different phenotypes in transgenic mutant PNKD vs. PNKD knock-out mice.

Dyskinesias as Synaptopathies. RIMs bind to voltage-gated calcium channels (N- and P/Q-type) directly with their PDZ domain and indirectly through the RIM binding protein (16, 29). In addition, RIM binding protein associates with L-, N-, and P/Q-type calcium channels in different cell types, and in vitro disruption of the association between calcium channel subunits and RIM binding protein results in enhanced release. More interestingly, mutations in P/Q-type voltage-gated calcium channel subunits are responsible for two other paroxysmal dyskinesia mouse models, *tottering* and *lethargic*. It is now intriguing to speculate that calcium-triggered neurotransmitter release may be the downstream homeostat and the site of malfunction in paroxysmal dyskinesias. Paroxysmal dyskinesia patients appear completely normal between attacks suggesting that homeostatic mechanisms regulating excitability are able to compensate much of the time. In presynaptic terminals, caffeine acts as a ryanodine receptor agonist and stimulates calcium efflux from the endoplasmic reticulum. We speculate that in mut-Tg mice, neurons are more vulnerable to elevated calcium levels and thus develop hyperexcitability when challenged with coffee, alcohol, or stress. In our mutant PNKD mouse model and other generalized dystonia mouse models, dysregulated dopamine signaling has been demonstrated in the striatum (10, 33–37).

Although proteins involved in neurotransmitter exocytosis are known to be important for vesicle release and neuronal signaling, they have yet to be implicated in episodic disorders. Another

form of dyskinesia, generalized dystonia, is caused by a gene encoding TorsinA, a novel AAA⁺ ATPase that resides in the endoplasmic reticulum. Like PNKD, the function of TorsinA is unknown. Our finding that Pnkd is a novel synaptic protein regulating RIM-dependent neurotransmitter release provides evidence supporting the role of genetic defects in synaptic function in the pathophysiology of dyskinesias. More recently, a related dyskinesia, paroxysmal kinesigenic dyskinesia with infantile convulsions (PKD/IC) was shown to be caused by mutations in proline-rich transmembrane protein 2 (PRRT2) (38). PRRT2 encodes a novel protein that interacts with SNAP25 (38, 39). The growing understanding of synaptic regulation and the role of synaptic dysregulation in paroxysmal dyskinesias will be important for developing better treatments for patients with many neurological diseases where altered synaptic physiology is the final common pathway in pathogenesis.

Episodic Disorders: Channelopathies and Beyond. When the first ion channel gene causing an episodic/electrical human disease was cloned in 1991, we predicted that homologous genes expressed in other tissues were likely to be responsible for other diseases like cardiac arrhythmias, peripheral nerve disorders, epilepsy, and migraine headache (40). Work from our laboratory and many others have now gone on to prove that this is indeed true (reviewed in refs. 3, 41, and 42). Mutations have been found in ion channel genes and cause many phenotypes, including periodic paralysis, long-QT syndrome, episodic ataxia, multiple forms of familial epilepsy, familial hemiplegic migraine, congenital insensitivity to pain, and erythromelalgia (a hypersensitivity/pain syndrome). Such genes include voltage-gated and ligand-gated ion channels, inwardly rectifying ion channels, ion exchangers, and transporters. This finding fits with the central roles that ion channels play as the primary determinants of membrane excitability.

However, it is also well known that channels are regulated by auxiliary subunits (e.g., β -subunits) and mutations in genes encoding such proteins can phenocopy some of these disorders (reviewed in ref. 43). Membrane excitability also depends on the trafficking and localization of channels in cells. Examples of mutations in such structural proteins are also known in disorders like long-QT syndrome (44). Channel function and membrane excitability is also affected by posttranslational modifications (e.g., phosphorylation). Thus, structural proteins important for trafficking/localization and proteins modifying channel function through posttranslational modifications can also phenocopy these electrical diseases (reviewed in ref. 45). There are also known examples where similar disorders can be acquired through development of autoantibodies directed against ion channels (reviewed in refs. 46 and 47).

The PNKD mouse model and the work presented here show that another class of episodic disorders can arise from dysregulation of signaling at synapses. It may be the case that with both PNKD and PKD/IC, that the channels and receptors involved are functioning completely normally but in a setting where synaptic function is altered, thus leading to abnormal signaling between neurons (48).

We outline a classification scheme for episodic/electrical disorders (Fig. 5). Channelopathies figure prominently in this scheme. Thus, we propose to limit the use of channelopathy only for electrical/episodic disorders when there is specific dysfunction of ion channels because of mutation in the genes encoding these proteins, for genes/proteins directly regulating ion channels through altered trafficking/localization or function (secondary channelopathies), or when autoantibodies are targeted against channels, thus altering their function (acquired channelopathies). The present paper and related work suggest that paroxysmal dyskinesias should be classified as synaptopathies. Much progress has been made in the last two decades since identification of the first channelopathy (40) leading up to this classification scheme (Fig. 5). Ongoing work will require modifications and refinements to this scheme as we learn more about the genetics and pathophysiology of this fascinating group of episodic/electrical disorders.

Experimental Procedures

Mouse Strains. The use and care of animals in this study follows the guidelines of the Institutional Animal Care and Use Committee at the University of California, San Francisco. *Mut-Tg* and *Pnkd*^{-/-} mice were generated as described previously (10). The founder mutant mice were backcrossed to C57BL/6 for 10 generations before used for experiments.

Plasmids and Antibodies. Full-length cDNA of human PNKD long form was previously described (49). Double mutations (A7V/A9V) were introduced into the human PNKD cDNA sequence by QuikChange XL Site-Directed Mutagenesis Kit (Stratagene). RIM1 and RIM2 clones are gifts from Thomas Südhof, Stanford Institute for Neuro-Innovation and Translational Neurosciences, Stanford University, Palo Alto, CA. Subclones of RIM1 and RIM2 were obtained by RT-PCR from mouse brain cDNA using Expanded High Fidelity PCR (Roche) and cloned into pCMV-Tag2B (Stratagene). The nucleotide sequence positions for RIM1 (NM_053270.1) subclones are Zinc Finger+PDZ 1-1600, C2A 1303-3007, C2B, 2887-4392; for RIM2 (NM_053271.1) subclones are Zinc Finger 1-2107, PDZ 1501-2400, C2A 2413-3630, C2B, 3635-4593. All constructs were sequence-confirmed.

A Rabbit antibody (C2235) was raised against the carboxyl-terminus peptide of PNKD, and against the N-terminal peptide (2226) (9). RIM antibody (BD Biosciences) recognizes both RIM1 and RIM2. Other antibodies include SNAP-25 (BD Biosciences), Flag, Munc13-1 (Sigma), Synaptotagmin, HGH, GFP (Abcam), GluR2, Synaptophysin, GAPDH (Chemicon), VAMP, Syntaxin1, Rab3, Munc18-1 (SySy), Rabphilin 3A, Synapsin 1 (ABR), PSD95 (New England Biolabs), and NR1 (Upstate).

Coimmunoprecipitation, Mass Spectrometry, and Western Blot. The frontal cortex of 2-mo-old C57BL/6 mice were removed rapidly and homogenized in RIPA buffer supplemented with benzonase nuclease (Novagen) and Complete protease inhibitors (Roche Applied Science). Soluble extracts were precleared by protein G agarose (Amersham Biosciences) for 4 h at 4 °C, then incubated together with either rabbit IgG or rabbit PNKD antibody and fresh protein G agarose overnight at 4 °C. Beads were washed five times with 0.1% Triton X-100 in PBS, and then bound protein was eluted using lithium dodecyl sulfate buffer (Invitrogen) and heated at 100 °C for 5 min. Elutions were resolved on 10% (wt/vol) SDS/PAGE gels and precipitated protein bands were visualized by SilverQuest (Invitrogen). The proteins that only precipitated in C57BL/6 sample but not in *Pnkd*^{-/-} sample were cut from

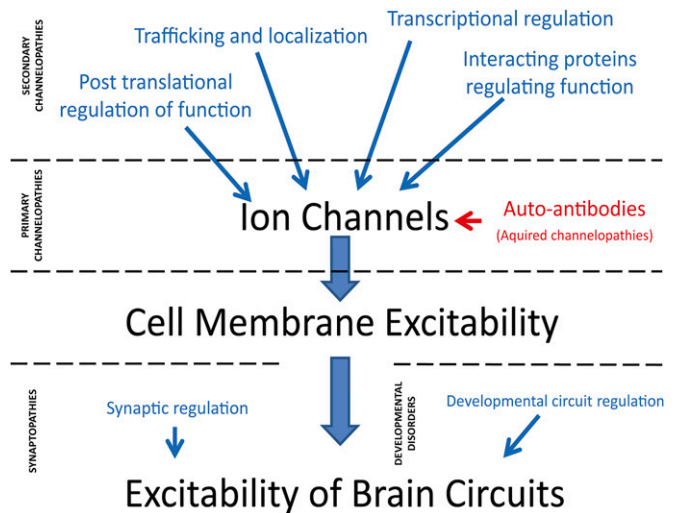


Fig. 5. Proposed classification scheme for episodic/electrical disorders. We propose that the term “channelopathy” be reserved for episodic/electrical disorders in which the genetic cause has been shown to be a mutation in an ion channel (primary channelopathy) or in proteins regulating trafficking/localization and regulation of ion channels (secondary channelopathies). Alternatively, acquired channelopathies can occur when autoantibodies are directed at ion channels. Paroxysmal dyskinesias appear to be caused (at least in PNKD and probably in PKD/IC) by dysfunction at the synapse (synaptopathies). Finally, developmental disorders affecting brain circuitry can give rise to hyperexcitability manifest, for example, as epilepsy. Reprinted, with permission, from ref. 57.

the gel and extracted using a standard peptide digestion and extraction protocol. Peptides were analyzed by MS/MS on an ABI 4700 MALDI-TOF/TOF and identified by blasting (www.expasy.org) database. For Western blots, protein samples were resolved on 10% SDS/PAGE gels, transferred to PVDF membranes (Millipore), and probed with antibody according to a standard Western blotting protocol (50). All coimmunoprecipitation were independently performed minimum of three times, and all mouse brain lysates are from 2- to ~3-mo-old male mice for a minimum of five mice. Western blots are quantitated by fluorescence (Odyssey, Li-Cor) and densitometry and normalized to GAPDH levels before comparison.

RIM Degradation Assay. SH-5Y5Y cell were cultured in regular DMEM containing 10% FBS. Cells were transfected with PNKD expression vector and RIM1 expression vectors by Lipofectamine 3000 reagent (Life Technologies). Forty-eight hours after the transfection, cells were treated with 100 g/mL cycloheximide (Thermo Scientific) for 4 or 7 h and harvested in SDS/PAGE sample buffer.

Electron Microscopy. Brain tissue from wild-type and *Pnkd*^{-/-} mice (*n* = 3 per genotype) was embedded in Lowicryl HM20 (Polysciences) using freeze substitution in methanol. Anesthetized mice were transcardially perfused with 0.1% glutaraldehyde (Roth) and 4% paraformaldehyde (Merck) in 0.1 M PB at 37 °C, and postfixed for 2 h. Next, 300- μ m-thick vibratome slices were infiltrated for cryoprotection with 5% sucrose in 0.1 M PB followed by 10%, 20%, and 30% glycerol in 0.1 M PB for 2 h each. Cortex blocks were cut and plunged into 4% uranylacetate in 99.5% methanol precooled to -90 °C in a Leica AFS2 for 12 h and additional 24 h at -45 °C (slope 5 °C/h). After three washing steps in methanol (30 min at -45 °C) infiltration followed for 2 h with 50% Lowicryl in methanol, 67% Lowicryl in methanol, and pure Lowicryl for additional 16 h. Polymerization with UV-light proceeded for 24 h at -45 °C followed by 24 h at 0 °C (slope 4 °C/h), and finally 24 h at room temperature (slope 0.9 °C/h). Postembedding immunogold labeling on Lowicryl sections started by blocking on 2% HSA/0.05 M TBS droplets, followed by incubation with anti-PNKD (No. 2226; 1:200) overnight at 4 °C, and 10-nm gold antibody for 2 h at room temperature. Labeled sections were washed in TBS, and contrasted with saturated uranylacetate. Samples were investigated with a transmission electron microscope (Libra 120, Zeiss) at 80 kV, and images taken with a 2048 × 2048 CCD camera (Tröndle).

Cell Culture and vGluT1-pH Imaging. Hippocampal CA3-CA1 neurons were cultured from P1 Sprague-Dawley rats as previously described (51). To test the role of PNKD on synaptic vesicle exocytosis or endocytosis, cultured hippocampal neurons were cotransfected with vesicular glutamate transporter1 fused with pH-sensitive GFP (vGluT1-pHluorin) (52) with wild-type or MUT PNKD-mKate constructs or empty vector control. Transfection was performed by the calcium phosphate method [days in vitro (DIV) 8 to DIV10] and neurons were studied between DIV14 and DIV19. Cotransfected neurons were identified by the colors of GFP and mKate. Neurons were stimulated with platinum electrodes and imaged at 1 Hz by a Cascade 512B camera using a standard GFP filter cube (Chroma) (53). To quantify the fluorescence signal of individual synaptic boutons, the regions of interest (circles with a diameter of 2 μ m) were manually placed over the center of fluorescent puncta, and three large regions of interest (diameter of 5~10 μ m) over the field without cell bodies or processes serve as background control.

To determine total vesicle pools, tyrode solution containing 50 mM NH₄Cl (pH 7.4) solution was perfused onto the neurons imaged at the end of experiments. The fluorescence signals in cotransfected boutons were averaged and subtracted from the average background, and the changes in fluorescence signals over time (ΔF) were normalized to the signal obtained by NH₄Cl perfusion. Data represents 100~200 boutons per coverslip and nine coverslips from three independent transfections. Imaging analysis was performed blinded to the constructs transfected and performed as previously described (54).

Slice Preparation and Electrophysiological Recordings of fEPSP. Hippocampal slices were prepared as described previously (55). In brief, after decapitation, the hippocampus (postnatal 21–28 d) was dissected rapidly and placed in ice-cold oxygenated (95% O₂–5% CO₂) Artificial cerebrospinal fluid solution containing: 124 mM NaCl, 5 mM KCl, 1.25 mM NaH₂PO₄, 1.3 mM MgCl₂, 2.6 mM CaCl₂, 26 mM NaHCO₃, 10 mM glucose, pH 7.4, 300–310 mOsm. Transverse slices (400 μ m thick) were cut with a vibratome and maintained in an incubation chamber for 2 h at 25 °C before recording. During experiments, an individual slice was transferred to a submersion recording chamber and was continuously perfused with the above-mentioned oxygenated solution (3.0 mL/min) at room temperature (22–25 °C). Current pulses (10–80 μ A, 100 μ s) were applied through concentric bipolar electrodes (MCE-100, RMI) placed at stratum radiatum in the CA1 region to induce fEPSP (56). fEPSPs were recorded from the dendrites of CA1 pyramidal cells using a glass electrode filled with normal artificial cerebrospinal fluid. The stimulus intensity for synaptic facilitation of 1, 5, and 10 Hz was set to generate a fEPSP with amplitude roughly 20–30% of the maximum response. Signals filtered at 5 kHz using the amplifier circuitry were sampled at 10 kHz and analyzed with Clampex 9.2 (Axon Instrument). fEPSP slopes were measured during the initial 1–1.5 ms of the fEPSP, and the averages of three subsequent responses were calculated. Synaptic facilitations were measured as the percentage of the fEPSP slope vs. the first fEPSP slope at a given stimulus train in individual slices (56).

Recording of mEPSC from Pyramidal Neurons. Whole-cell patch-clamp recordings were made from pyramidal neurons in layer 2–3 motocortex in the presence of γ -aminobutyric acid type A antagonist picrotoxin (50 μ M) and sodium channel block TTX (0.5 μ M). Recording pipettes were routinely filled with a solution containing: 125 mM K-gluconate, 15 mM KCl, 10 mM Hepes, 8 mM NaCl, 3 mM Na₂ATP, 0.3 mM Na-GTP, 10 mM Na₂-phosphocreatine, and 0.2 mM EGTA (290–300 mOsm, pH 7.3 adjusted with KOH). Membrane potential of the neurons was held at -70 mV. Spontaneous mEPSCs in neurons were recorded under a gap-free mode. The data were analyzed by Mini Analysis Program, Synaptosoft.

ACKNOWLEDGMENTS. We thank Dr. Devon Ryan for critical reading of the manuscript; Drs. Robert Edwards, Pascal Kaeser, and Thomas Südhof for helpful discussions; Drs. Yun Wang, Pascal Kaeser, and Thomas Südhof for their generous gifts of RIM plasmids and RIM knockout mouse strains; and Drs. Yongling Zhu and Chen Zhang for helpful suggestions. This work is supported by NIH Grant U54 RR19481, the Bachmann-Strauss Dystonia & Parkinson Foundation (L.J.P.), the Sandler Neurogenetics Fund, and a postdoctoral fellowship from the Dystonia Medical Research Foundation (to Y.S. and L.J.P.). L.J.P. and L.Y.J. are investigators of the Howard Hughes Medical Institute.

- Mount LA, Reback S (1940) FAMILIAL PAROXYSMAL CHOREOATHETOSIS preliminary report on a hitherto undescribed clinical syndrome. *Arch Neurol Psychiatry* 44(4):841–847.
- Bruno MK, et al. (2007) Genotype-phenotype correlation of paroxysmal nonkinesigenic dyskinesia. *Neurology* 68(21):1782–1789.
- Ryan DP, Ptáček LJ (2010) Episodic neurological channelopathies. *Neuron* 68(2):282–292.
- Fureman BE, Jinnah HA, Hess EJ (2002) Triggers of paroxysmal dyskinesia in the calcium channel mouse mutant *tottering*. *Pharmacol Biochem Behav* 73(3):631–637.
- Neychev VK, Fan X, Mitev VI, Hess EJ, Jinnah HA (2008) The basal ganglia and cerebellum interact in the expression of dystonic movement. *Brain* 131(Pt 9):2499–2509.
- Pizoli CE, Jinnah HA, Billingsley ML, Hess EJ (2002) Abnormal cerebellar signaling induces dystonia in mice. *J Neurosci* 22(17):7825–7833.
- Burgess DL, Jones JM, Meisler MH, Noebels JL (1997) Mutation of the Ca²⁺ channel beta subunit gene *Cchb4* is associated with ataxia and seizures in the *lethargic* (lh) mouse. *Cell* 88(3):385–392.
- Fletcher CF, et al. (1996) Absence epilepsy in tottering mutant mice is associated with calcium channel defects. *Cell* 87(4):607–617.
- Lee HY, et al. (2004) The gene for paroxysmal non-kinesigenic dyskinesia encodes an enzyme in a stress response pathway. *Hum Mol Genet* 13(24):3161–3170.
- Lee HY, et al. (2012) Dopamine dysregulation in a mouse model of paroxysmal nonkinesigenic dyskinesia. *J Clin Invest* 122(2):507–518.
- Südhof TC (2004) The synaptic vesicle cycle. *Annu Rev Neurosci* 27:509–547.
- Wang Y, Südhof TC (2003) Genomic definition of RIM proteins: Evolutionary amplification of a family of synaptic regulatory proteins. *Genomics* 81(2):126–137.
- Castillo PE, Schoch S, Schmitz F, Südhof TC, Malenka RC (2002) RIM1alpha is required for presynaptic long-term potentiation. *Nature* 415(6869):327–330.
- Kaeser PS, Südhof TC (2005) RIM function in short- and long-term synaptic plasticity. *Biochem Soc Trans* 33(Pt 6):1345–1349.
- Kaeser PS, et al. (2008) RIM1alpha and RIM1beta are synthesized from distinct promoters of the RIM1 gene to mediate differential but overlapping synaptic functions. *J Neurosci* 28(50):13435–13447.
- Kaeser PS, et al. (2011) RIM proteins tether Ca²⁺ channels to presynaptic active zones via a direct PDZ-domain interaction. *Cell* 144(2):282–295.
- Schoch S, et al. (2002) RIM1alpha forms a protein scaffold for regulating neurotransmitter release at the active zone. *Nature* 415(6869):321–326.
- Wang Y, Okamoto M, Schmitz F, Hofmann K, Südhof TC (1997) Rim is a putative Rab3 effector in regulating synaptic-vesicle fusion. *Nature* 388(6642):593–598.
- Schoch S, et al. (2006) Redundant functions of RIM1alpha and RIM2alpha in Ca(2+)-triggered neurotransmitter release. *EMBO J* 25(24):5852–5863.
- Turnbull J, et al. (2005) Sacred disease secrets revealed: The genetics of human epilepsy. *Hum Mol Genet* 14(17):2491–2500.
- Betz A, et al. (2001) Functional interaction of the active zone proteins Munc13-1 and RIM1 in synaptic vesicle priming. *Neuron* 30(1):183–196.
- Deng L, Kaeser PS, Xu W, Südhof TC (2011) RIM proteins activate vesicle priming by reversing autoinhibitory homodimerization of Munc13. *Neuron* 69(2):317–331.

23. Dulubova I, et al. (2005) A Munc13/RIM/Rab3 tripartite complex: From priming to plasticity? *EMBO J* 24(16):2839–2850.
24. Koushika SP, et al. (2001) A post-docking role for active zone protein Rim. *Nat Neurosci* 4(10):997–1005.
25. Deken SL, et al. (2005) Redundant localization mechanisms of RIM and ELKS in *Caenorhabditis elegans*. *J Neurosci* 25(25):5975–5983.
26. Kaeser PS, et al. (2009) ELKS2alpha/CAST deletion selectively increases neurotransmitter release at inhibitory synapses. *Neuron* 64(2):227–239.
27. Wang Y, Liu X, Biederer T, Südhof TC (2002) A family of RIM-binding proteins regulated by alternative splicing: Implications for the genesis of synaptic active zones. *Proc Natl Acad Sci USA* 99(22):14464–14469.
28. Han Y, Kaeser PS, Südhof TC, Schneggenburger R (2011) RIM determines Ca²⁺ channel density and vesicle docking at the presynaptic active zone. *Neuron* 69(2):304–316.
29. Hibino H, et al. (2002) RIM binding proteins (RBPs) couple Rab3-interacting molecules (RIMs) to voltage-gated Ca(2+) channels. *Neuron* 34(3):411–423.
30. Coppola T, et al. (2001) Direct interaction of the Rab3 effector RIM with Ca²⁺ channels, SNAP-25, and synaptotagmin. *J Biol Chem* 276(35):32756–32762.
31. Kiyonaka S, et al. (2007) RIM1 confers sustained activity and neurotransmitter vesicle anchoring to presynaptic Ca²⁺ channels. *Nat Neurosci* 10(6):691–701.
32. Yao I, et al. (2007) SCRAPPER-dependent ubiquitination of active zone protein RIM1 regulates synaptic vesicle release. *Cell* 130(5):943–957.
33. DeLong MR, Wichmann T (2007) Circuits and circuit disorders of the basal ganglia. *Arch Neurol* 64(1):20–24.
34. Jinnah HA, et al. (2005) Rodent models for dystonia research: Characteristics, evaluation, and utility. *Mov Disord* 20(3):283–292.
35. Kaji R (2001) Basal ganglia as a sensory gating device for motor control. *J Med Invest* 48(3–4):142–146.
36. Shirley TL, Rao LM, Hess EJ, Jinnah HA (2008) Paroxysmal dyskinesias in mice. *Mov Disord* 23(2):259–264.
37. Wichmann T (2008) Commentary: Dopaminergic dysfunction in DYT1 dystonia. *Exp Neurol* 212(2):242–246.
38. Lee HY, et al. (2012) Mutations in the gene PRRT2 cause paroxysmal kinesigenic dyskinesia with infantile convulsions. *Cell Reports* 1(1):2–12.
39. Stelzl U, et al. (2005) A human protein-protein interaction network: A resource for annotating the proteome. *Cell* 122(6):957–968.
40. Ptáček LJ, et al. (1991) Identification of a mutation in the gene causing hyperkalemic periodic paralysis. *Cell* 67(5):1021–1027.
41. Ryan DP, Ptáček LJ (2007) Channelopathies. *The Molecular & Genetic Basis of Neurological & Psychiatric Disease*, eds Rosenberg RN, DiMauro S, Paulson HL, Ptáček L, Nestler EJ (Lippincott, Williams & Wilkins, New York), 4th Ed.
42. Russell JF, Fu YH, Ptáček LJ (2013) Episodic neurologic disorders: Syndromes, genes, and mechanisms. *Annu Rev Neurosci* 36:25–50.
43. O'Malley HA, Isom LL (2015) Sodium channel β subunits: Emerging targets in channelopathies. *Annu Rev Physiol* 77:481–504.
44. Mohler PJ, et al. (2003) Ankyrin-B mutation causes type 4 long-QT cardiac arrhythmia and sudden cardiac death. *Nature* 421(6923):634–639.
45. Curran J, Mohler PJ (2015) Alternate paradigms for ion channelopathies: Disorders of ion channel membrane trafficking and posttranslational modification. *Annu Rev Physiol* 77:505–524.
46. Irani SR, Gelfand JM, Al-Diwani A, Vincent A (2014) Cell-surface central nervous system autoantibodies: Clinical relevance and emerging paradigms. *Ann Neurol* 76(2):168–184.
47. Vincent A (2013) Developments in autoimmune channelopathies. *Autoimmun Rev* 12(6):678–681.
48. Lee H-Y, Fu Y-H, Ptáček LJ (2015) Episodic and electrical nervous system disorders caused by nonchannel genes. *Annu Rev Physiol* 77:525–541.
49. Shen Y, et al. (2011) Mutations in PNKD causing paroxysmal dyskinesia alters protein cleavage and stability. *Hum Mol Genet* 20(12):2322–2332.
50. Shen Y, Lee G, Choe Y, Zoltewicz JS, Peterson AS (2007) Functional architecture of atrophins. *J Biol Chem* 282(7):5037–5044.
51. Liu G, Tsien RW (1995) Synaptic transmission at single visualized hippocampal boutons. *Neuropharmacology* 34(11):1407–1421.
52. Voglmaier SM, et al. (2006) Distinct endocytic pathways control the rate and extent of synaptic vesicle protein recycling. *Neuron* 51(1):71–84.
53. Pyle JL, Kavalali ET, Piedras-Renteria ES, Tsien RW (2000) Rapid reuse of readily releasable pool vesicles at hippocampal synapses. *Neuron* 28(1):221–231.
54. Zhang Q, Li Y, Tsien RW (2009) The dynamic control of kiss-and-run and vesicular reuse probed with single nanoparticles. *Science* 323(5920):1448–1453.
55. Ge WP, Duan S (2007) Persistent enhancement of neuron-glia signaling mediated by increased extracellular K⁺ accompanying long-term synaptic potentiation. *J Neurophysiol* 97(3):2564–2569.
56. Zhang C, et al. (2009) Presenilins are essential for regulating neurotransmitter release. *Nature* 460(7255):632–636.
57. Ptáček LJ (2015) Episodic disorders: Channelopathies and beyond. *Annu Rev Physiol* 77:475–479.